Thoracic Cancer

WILEY

ORIGINAL ARTICLE OPEN ACCESS

Effects of Autophagy Inhibition by SAR405, a Selective VPS34 Inhibitor, on Pleural Mesothelioma Cells

Yoshiki Kuwabara | Kosuke Sakai | Kota Shiraishi | Itsuka Matsumoto | Shigeru Ishii | Shin Yokosuka | Masatoshi Abe | Tomoyuki Takahashi | Yuichiro Kawano | Hiroaki Nishimura | Maiko Toda-Sasaki | Yumiko Kobayashi-Ogawa | Satoshi Kikuchi | Yusuke Hirata | Hiroyuki Kyoyama | Gaku Moriyama | Nobuyuki Koyama | Kazutsugu Uematsu

Department of Pulmonary Medicine, Saitama Medical Center, Saitama Medical University, Saitama, Japan

Correspondence: Kazutsugu Uematsu (kuematsu@saitama-med.ac.jp)

Received: 8 July 2025 | **Revised:** 25 January 2026 | **Accepted:** 11 February 2026

Keywords: apoptosis | cisplatin | macroautophagy | pleural mesothelioma | SAR405 | VPS34

ABSTRACT

Background: Pleural mesothelioma is a highly aggressive malignancy with a poor prognosis due to the limited efficacy of currently available therapies. Macroautophagy (hereafter "autophagy") is a lysosome-mediated degradation pathway involved in cellular homeostasis that can either support or inhibit cancer progression depending on context. In this study, we investigated the effects of SAR405, an inhibitor of vacuolar protein-sorting 34 (VPS34), which is important for regulating the early stage of autophagy, on pleural mesothelioma.

Methods: Human pleural mesothelioma cell lines H28, H2452, and 211H were cultured with SAR405. The effects of SAR405 on protein expression, cell viability, colony formation, cell invasion, and the cell cycle were investigated, as were its synergistic effects with cisplatin. Autophagy induction was evaluated in mesothelioma cells transfected with the pMRX-IP-GFP-LC3-RFP-LC3ΔG plasmid, which was developed for the quantitative and statistical estimation of autophagy.

Results: SAR405 treatment alone significantly reduced cell viability, colony formation, and cell invasion, and increased G_2/M cell cycle arrest. In addition, SAR405 induced apoptosis in the H2452 cell line. Although cisplatin weakly induced autophagy in mesothelioma cells, its combination with SAR405 did not result in additive or synergistic effects on cell viability.

Conclusions: Based on these results, inhibition of VPS34 by SAR405 effectively suppressed cell viability in all mesothelioma cell lines and induced apoptosis in H2452 cells. The findings of this study indicate the potential for VPS34 inhibition as a new strategy for the treatment of mesothelioma and provide insights into the complex role of autophagy in this malignancy.

1 | Introduction

Pleural mesothelioma, which is primarily attributed to asbestos exposure, is currently treated with chemotherapy, radiotherapy, or immune checkpoint inhibitors; however, the prognosis remains poor. In Japan, it is estimated that more than 40 000 people will develop pleural mesothelioma between 2030 and 2039 [1]. Therefore, the development of effective therapies based on the molecular biology of mesothelioma is urgently required.

Macroautophagy (hereafter "autophagy") is a process by which cells capture intracellular proteins, lipids, and organelles and deliver them to the lysosomal compartment for degradation [2, 3]. The products of the autophagic degradation of intracellular material are exported from lysosomes into the cytoplasm, where they are recycled [4]. The intracellular recycling function of autophagy has variable effects on cellular and organismal physiology, depending on the circumstances. There is a long-term need for autophagy to prevent tissue damage and disease, as well as

This is an open access article under the terms of the Creative Commons Attribution License, which permits use, distribution and reproduction in any medium, provided the original work is properly cited.

© 2026 The Author(s). *Thoracic Cancer* published by John Wiley & Sons Australia, Ltd.

an acute requirement for autophagy to maintain homeostasis in stressful environments [5].

It is well known that autophagy acts as a double-edged sword in cancer [6]. In early carcinogenesis, autophagy has a tumor suppressor role because it prevents genomic instability by the induction of senescence [6]. As the tumor progresses, autophagy plays a tumor promoter role as it helps tumor cells to survive under conditions of microenvironmental stress, such as hypoxia, nutrient deprivation, and chemotherapy-induced stress [7]. In addition, autophagy has been associated with tumor metastasis, growth, and chemoresistance [8–10]. In contrast, a pro-death role of autophagy in response to high levels of stress and complex cross-talk between autophagy and apoptotic cell death have been reported [11, 12].

The autophagy pathway can be targeted by using various autophagy inhibitors. Chloroquine and hydroxychloroquine inhibit lysosomal acidification and autophagosome–lysosome fusion [4, 5]. Hydroxychloroquine is used in various medical specialties for long-term treatment, especially in clinical trials for cancer treatment. However, the use of hydroxychloroquine is associated with a significant risk of irreversible blindness due to hydroxychloroquine retinopathy, the prevalence of which has been reported to be as high as 7.5% [13], using recently developed and more sensitive diagnostic techniques. Moreover, hydroxychloroquine retinopathy may progress even after cessation of therapy [14, 15]. Therefore, clinically useful and novel autophagy inhibitors need to be developed.

In a previous study, we investigated the effect of VER-155008, which inhibits HSP70 function, on pleural mesothelioma [16]. In that study, VER-155008 suppressed the proliferation of pleural mesothelioma cells and induced autophagy. However, it was unclear whether the induction of autophagy observed in that study had cytotoxic or cytoprotective effects on cancer cells.

Therefore, the aim of the present study was to determine the role of autophagy in pleural mesothelioma cells by inhibiting autophagy using SAR405, a novel and highly potent autophagy inhibitor that selectively targets vacuolar protein-sorting 34 (VPS34). In addition, the effect of autophagy inhibition with SAR405 was examined in combination with cisplatin, a conventional therapeutic agent used for the treatment of pleural mesothelioma.

2 | Methods

2.1 | Cell Lines and Chemical Reagents

Human pleural mesothelioma cell lines 211H, H2452, and H28 (all from American Type Culture Collection, Manassas, VA, USA) were cultured in RPMI 1640 medium (SH30027.01; GE HealthCare, Tokyo, Japan) supplemented with 10% fetal bovine serum (Sigma-Aldrich, St. Louis, MO, USA) and 1% penicillin–streptomycin (168–23191; FUJIFILM Wako Pure Chemical, Osaka, Japan) at 37°C under 5% CO2. SAR405 (28012; MedChemExpress, Monmouth Junction, NJ, USA), PIK-III (22452; MedChemExpress), Vps34-IN-1 (24001; MedChemExpress), chloroquine diphosphate (28916; Sigma-Aldrich), cisplatin (033–20091; FUJIFILM Wako Pure Chemical), and/or dimethyl sulfoxide (DMSO; 046–21981; FUJIFILM Wako Pure Chemical), as a control, were added to the cell culture media. SAR405, PIK-III, and Vps34-IN-1 were dissolved in DMSO to a stock concentration of 1 mM, while cisplatin was dissolved in 0.9% sodium chloride solution to a stock concentration of 1.34 mM. In this study, RPMI-1640 was used for all experiments and the culture conditions were 37°C under 5% CO2.

2.2 | Western Blotting Analysis

Cells were lysed with the M-PER Mammalian Protein Extraction Reagent (YH371252; Thermo Fisher Scientific, Pittsburgh, PA, USA) according to the manufacturer's instructions. Cell lysates were mixed with 4× Laemmli sample buffer (161–0747; Bio-Rad, Hercules, CA, USA) containing 5% 2-mercaptoethanol (161–0737; Bio-Rad). Then, 30-μg aliquots were boiled at 95°C and separated by sodium dodecyl sulfate–polyacrylamide gel electrophoresis (4561094; Mini-PROTEAN TGX Gels; Bio-Rad). After incubation with 5% skim milk powder (LEE0023; FUJIFILM Wako Pure Chemical), blots were incubated for 24 h at 4°C with primary antibodies (diluted 1:1000 with Tris-buffered saline Tween-20 [TBS-T]). After washing with TBS-T, the blots were then incubated for 2 h at room temperature with the secondary antibody (diluted 1:50000 with TBS-T). After washing with TBS-T, antigen–antibody complexes were detected using a ChemiDoc XRS+ System (Bio-Rad) and SuperSignal West Femto (XF346244; Thermo Fisher Scientific).

The primary antibodies used in this study were as follows: caspase-3 rabbit polyclonal antibody (pAb; 9662), cleaved caspase-9 (Asp315) rabbit pAb (9505), poly (ADP-ribose) polymerase (PARP) rabbit pAb (9542), glyceraldehyde-3-phosphate dehydrogenase (GAPDH; D16H11) rabbit mAb (5174), and LC3B (D11) rabbit mAb (3868; all from Cell Signaling, Beverly, MA, USA); and p62 (sequestosome 1) rabbit pAb (PM045; MBL, Chiba, Japan). The secondary antibody was horseradish peroxidase (HRP)-conjugated anti-rabbit IgG (SA00001-2; Cosmo Bio, Tokyo, Japan).

2.3 | Cell Viability Analysis

Mesothelioma cells were seeded onto 96-well plates at a density of 1000 cells/well and cultured overnight. The medium was then changed to one containing 0.1–50 μM SAR405, 0.1–50 μM cisplatin, or DMSO as a control and cells were cultured for a further 72 h. Then, 10.0 μL Cell Counting Kit-8 reagent (CK04; Dojindo, Kumamoto, Japan) was added to each well and cells were cultured for 2 h. The number of viable cells was evaluated by measuring reduced water-soluble tetrazolium 8 (WST-8) at 450 nm (SH1300-Lab instrument; Hitachi High-Tech Science Corporation, Tokyo, Japan).

2.4 | Colony Formation

Mesothelioma cells were seeded onto 6-well plates at a density of 1000 cells/well and cultured overnight. The medium was then changed to one containing 2.5–5.0 μM SAR405 or DMSO

as a control and cells were cultured for 10 days in 211H and for 14 days in H28 and H2452, after which the colonies formed were stained with methylene blue (A334; Sigma-Aldrich) for counting.

2.5 | Cell Migration and Motility Assay

Cell invasion was measured using a scratch wound healing assay. Mesothelioma cells were seeded onto 6-well plates at a density of 1.2×10^5 cells/well. After 48 h incubation, the cell monolayer in each well was scraped with the tip of a sterile 100-μL pipette. The cells were then gently washed with medium to remove detached cells, after which the medium was replaced with fresh medium containing either 10.0 μM SAR405 or DMSO as a vehicle control. This medium replacement was designated as the 0 h time point for subsequent analyses. Images were taken at 0 and 48 h using a fluorescence microscope (BZ-X810 equipped with BZ series application 01.01.00.17; Keyence, Osaka, Japan). Cell migration and motility was assessed as a "closure rate", which was calculated by dividing the wound area at each time point by the original wound area.

2.6 | Cell Cycle and Apoptosis Analyses

Mesothelioma cells were seeded onto 6-well plates at a density of 1.2×10^5 cells/well. After overnight incubation, the medium was changed to one containing 2.5–10.0 μM SAR405 or DMSO as a control. After 48 h in culture, cells were used for cell cycle analysis or analysis of cell apoptosis. For cell cycle analysis, cells were stained with Cell Cycle Assay Solution Deep Red (VG508; Dojindo), and the proportion of cells in each phase of the cell cycle was determined by using a BD FACSVerse equipped with FACSuite v1.0.5.3841 (BD Biosciences, San Jose, CA, USA). To analyze cell apoptosis, cells were stained with annexin V–fluorescein isothiocyanate (FITC) and propidium iodide (IM2375; Beckman Coulter, Brea, CA, USA) according to the manufacturer's instructions, and stained cells were analyzed using the BD FACSVerse.

2.7 | Morphological Apoptosis

Cells were seeded onto 24-well plates at a density of 1.5×10^4 cells/well and cultured overnight. The medium was then changed to one containing 10 μM SAR405 or DMSO as a control. Cells were exposed to 10 μM SAR405 for 48 h, stained with Hoechst 33 342 for 20 min at 37°C, and observed under a fluorescence microscope (BZ-X810; Keyence).

2.8 | Autophagy Analysis

For evaluation of autophagy, mesothelioma cells were transfected with the pMRX-IP-GFP-LC3-RFP-LC3ΔG plasmid, as described previously [16, 17]. Transfected cells express GFP-LC3-RFP-LC3ΔG, which is cleaved by the autophagy-regulating protease ATG4 into GFP-LC3 and RFP-LC3ΔG. GFP-LC3 labels autophagosomes and is degraded by lysosomes during autophagy, resulting in a decrease in green fluorescence. In contrast, the red fluorescence of RFP-LC3ΔG remains stable, meaning it serves as an internal control. A decrease in the ratio of green fluorescent protein (GFP) to red fluorescent protein (RFP) indicates activation of autophagy.

Transfected mesothelioma cells were seeded onto 6-well plates and cultured overnight. The medium was then changed to one containing 0.5–5.0 μM cisplatin, 2.5–10.0 μM SAR405, or DMSO. After a further 24 h culture, the medium was removed and the cells were fixed with methanol and observed under a fluorescence microscope (BZ-X810; Keyence). Fluorescence intensity was measured (BD FACSVerse) as FITC for green fluorescence and phycoerythrin-Cy5 A (PC5-A) for red fluorescence. Mean green and red fluorescence values were assessed, and autophagy activity was assessed on the basis of the GFP/RFP ratio.

2.9 | Spheroid Culture and Projected Area Measurement

Mesothelioma cells were seeded onto an Akura 96 Spheroid Microplate (25 071 608 AU; InSphero, Schlieren, Switzerland) at densities of 4500 cells/well for H28, 3000 cells/well for H2452, and 2000 cells/well for 211H. After 72 h of spheroid formation, the culture medium was changed to 5.0–10.0 μM SAR405, or DMSO. Following an additional 72 h of incubation, spheroids were imaged using a ZOE Fluorescent Cell Imager (Bio-Rad), and spheroid size was quantified as projected area using ImageJ software (version 1.54 g; National Institutes of Health, Bethesda, MD, USA) [18].

2.10 | Statistical Analysis

Statistical analyses were performed using EZR version 2.5–1 (Saitama Medical Center, Jichi Medical University, Saitama, Japan) [19]. The significance of differences between two groups was determined using *F* tests and *t*-tests. For multiple comparisons, Dunnett's multiple comparisons test was used to compare each group with the control group. All data are expressed as the mean ± SD of three independent experiments, and the level of significance was set at two tailed $p < 0.05$.

The effects of combining two drugs were evaluated using SynergyFinder version 3.0 in R [20], and zero interaction potency (ZIP) values. Based on the ZIP synergy scoring model, the delta (Δ%) scores were interpreted as follows: less than −10, antagonistic; between −10 and 10, additive; and above 10, synergistic.

3 | Results

3.1 | Effects of SAR405 on Autophagy in Pleural Mesothelioma Cells

Fluorescence microscopy revealed that, in all mesothelioma cell lines (H28, H2452, and 211H) that were transfected with the pMRX-IP-GFP-LC3-RFP-LC3ΔG plasmid, the addition of SAR405 to the culture medium increased GFP-LC3 fluorescence compared with control (Figure 1A). Flow cytometry, which quantitatively measured GFP and RFP fluorescence intensities, revealed that

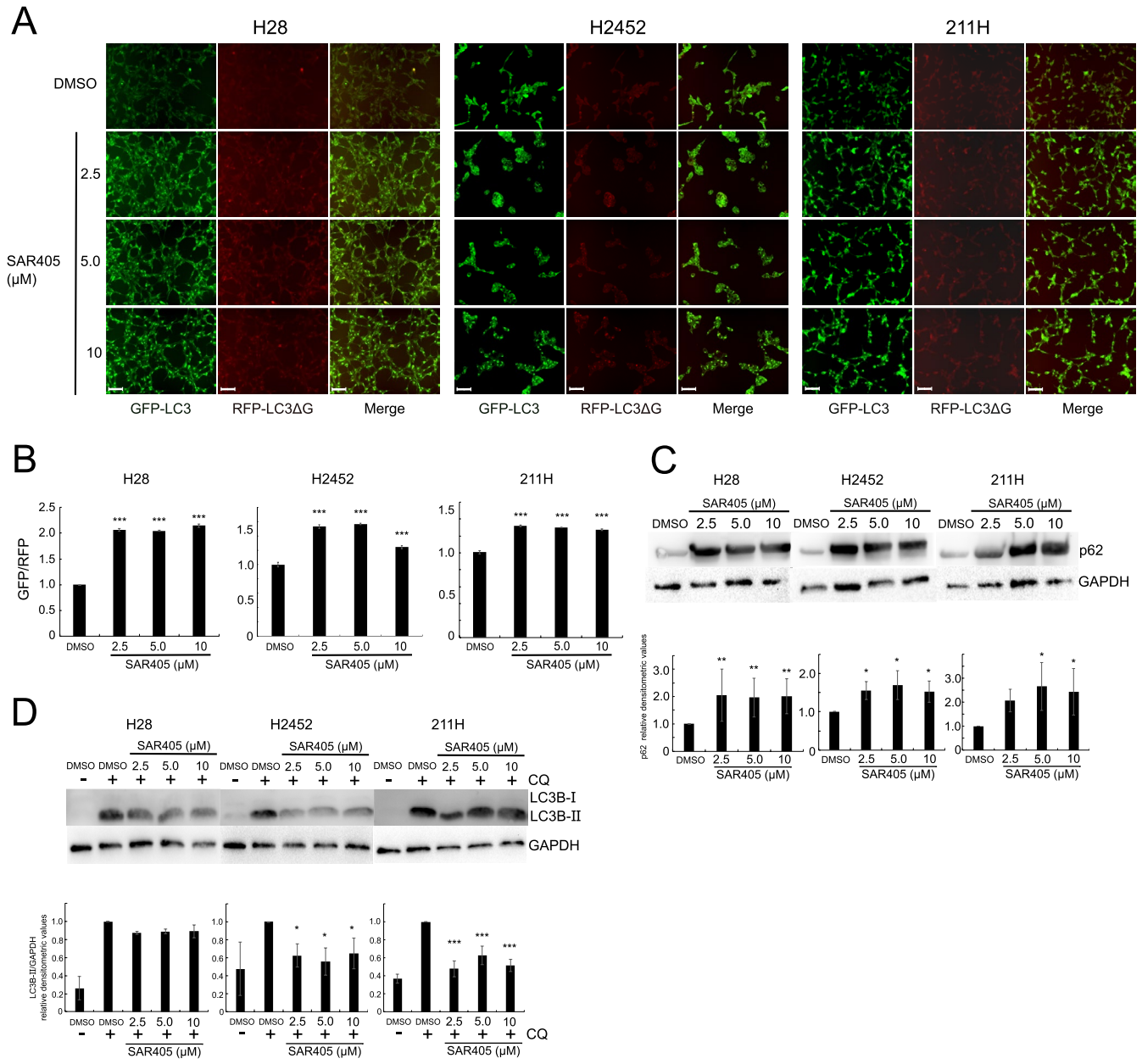


FIGURE 1 | Suppression of autophagy in pleural mesothelioma cells by SAR405, a VPS34 inhibitor. To evaluate autophagy, mesothelioma cells were transfected with the pMRX-IP-GFP-LC3-RFP-LC3ΔG plasmid and then cultured for 24 h with 2.5–10.0 μM SAR405 or dimethyl sulfoxide (DMSO) as a control. (A) Fluorescence microscopy findings. Scale bars = 200 μm. (B) Signal intensities of green fluorescent protein (GFP) and red fluorescent protein (RFP) were measured by flow cytometry and the GFP/RFP ratio was used as an indicator of autophagy activation. (C) Western blotting analysis of p62 expression (as a marker of autophagy). GAPDH, glyceraldehyde-3-phosphate dehydrogenase. (D) Effects of 10.0 μM chloroquine (CQ), alone and in the presence of 2.5–10.0 μM SAR405, on LC3B levels in mesothelioma cells, as determined by western blotting analysis, with GAPDH used as a loading control. Data are presented as the mean ± SD of three independent experiments. *$p < 0.05$, **$p < 0.01$, ***$p < 0.001$ compared with DMSO.

SAR405 at concentrations ≥ 2.5 μM increased the GFP/RFP ratio in all pleural mesothelioma cell lines (Figure 1B). These findings indicate that SAR405 suppressed autophagy in these mesothelioma cell lines. Using the conventional method for the evaluation of autophagy, namely degradation of p62/sequestosome 1 (an autophagy marker) as detected by western blotting analysis, also demonstrated autophagy suppression by SAR405 (Figure 1C).

Because the steady state level of autophagosomes is determined by the balance between their synthesis and consumption in lysosomes, inhibiting autophagosome consumption with chloroquine, a lysosomotropic drug that affects lysosome function by increasing pH, can be used to determine whether a drug truly inhibits autophagy or merely induces it. In this study, chloroquine induced the accumulation of LC3B-II in all cell lines. In H2452 and 211H cells, the addition of SAR405 significantly inhibited the chloroquine-induced accumulation of LC3B-II compared with DMSO + chloroquine as a control. In H28 cells, although there was a tendency for SAR405 to inhibit chloroquine-induced accumulation of LC3B-II compared with control, the difference was not statistically significant (Figure 1D).

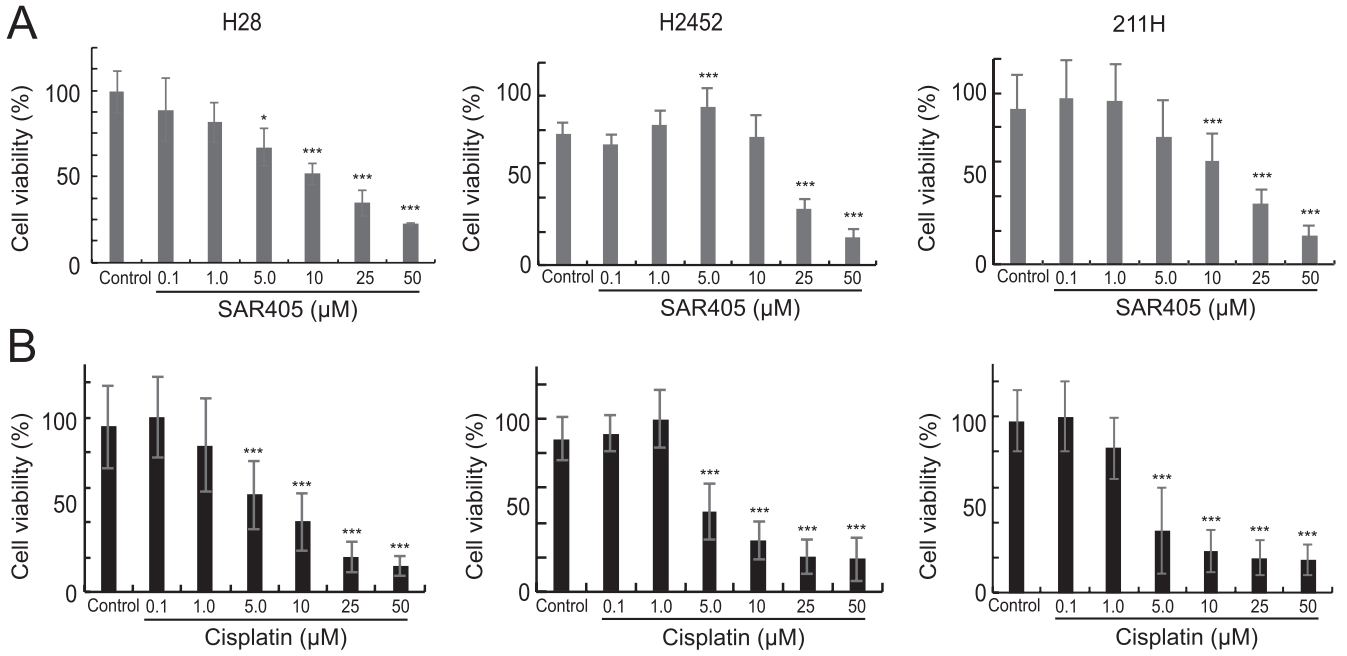


FIGURE 2 | Effects of (A) SAR405 and (B) cisplatin on the cell viability of pleural mesothelioma cells. Cell viability was assessed by measuring the reduction of water-soluble tetrazolium 8 (WST-8). Data are the mean ± SD of three independent experiments. *$p < 0.05$, ***$p < 0.001$ compared with control.

3.2 | Effects of SAR405 on the Cell Viability of Pleural Mesothelioma Cells

To investigate the effects of SAR405 on the cell viability of pleural mesothelioma cells, the IC_{50} for SAR405 was determined and compared to that for cisplatin, which is conventionally used for the treatment of malignant pleural mesothelioma. After 72 h exposure to SAR405, cell viability of H28, H2452, and 211H cells was suppressed by SAR405 at concentrations of ≥ 5.0, ≥ 25.0, and ≥ 10.0 μM, respectively. The IC_{50} for SAR405 at 72 h was 10.8 μM for H28 cells, 17.4 μM for H2452 cells, and 12.4 μM for 211H cells (Figure 2A). Meanwhile, cisplatin significantly inhibited cell proliferation at concentrations ≥ 5 μM in all cell lines. The IC_{50} value for cisplatin at 72 h was 4.6 μM for H28 cells, 7.6 μM for H2452 cells, and 3.2 μM for 211H cells (Figure 2B).

3.3 | Effects of SAR405 on Colony Formation and Cell Invasion

SAR405 inhibited colony formation at a concentration of 2.5 μM in H28 cells and 5.0 μM in H2452 and 211H cells (Figure 3).

In scratch wound healing assay, microscopy revealed that cell migration was suppressed by 10.0 μM SAR405 in all pleural mesothelioma cell lines compared with control (DMSO) after 48 h (Figure 4A). Forty-eight hours after creation of the wound area in mesothelioma cell monolayers, the respective areas remaining in the control (DMSO) and SAR405 groups were 13.9% and 74.9% for H28 cells, 36.6% and 82.9% for H2452 cells, and 27.0% and 84.6% for 211H cells (Figure 4B).

3.4 | Effects of SAR405 on the Cell Cycle and Apoptosis in Pleural Mesothelioma Cells

It has been reported that the antitumor effects of various therapeutic agents on pleural mesothelioma cells are accompanied by cell cycle arrest at the G_2/M phase [21]. In the present study, the G_2/M phase cell population increased after 24 h of culture of H28, H2452, and 211H cells with 2.5–10.0 μM SAR405 versus DMSO (Figure 5).

Cell cycle analysis showing an increase in the sub-G_1 population of mesothelioma cells compared to the control (DMSO) group suggested the induction of apoptosis. After 24 h of treatment with 10.0 μM SAR405, Hoechst 33 342 staining of H2452 cells revealed apoptotic morphology, including cell shrinkage, chromatin condensation, and nuclear fragmentation (Figure 6A). Western blotting analysis revealed that the treatment of H2452 cells with 10.0 μM SAR405 induced PARP, cleaved caspase-3, and cleaved caspase-9 expression (Figure 6B), all of which are markers of apoptosis induction. These results confirm the induction of apoptosis by SAR405 in H2452 cells. Flow cytometry analysis with annexin V-FITC/propidium iodide staining demonstrated a significant increase in apoptosis in H2452 cells treated with 10.0 μM SAR405, whereas no such increase was seen in H28 and 211H cells (Figure 6C).

3.5 | Effects of Cisplatin on Autophagy in Pleural Mesothelioma Cells

Before evaluating the combined effects of SAR405 and cisplatin, a conventional therapeutic agent for the treatment of

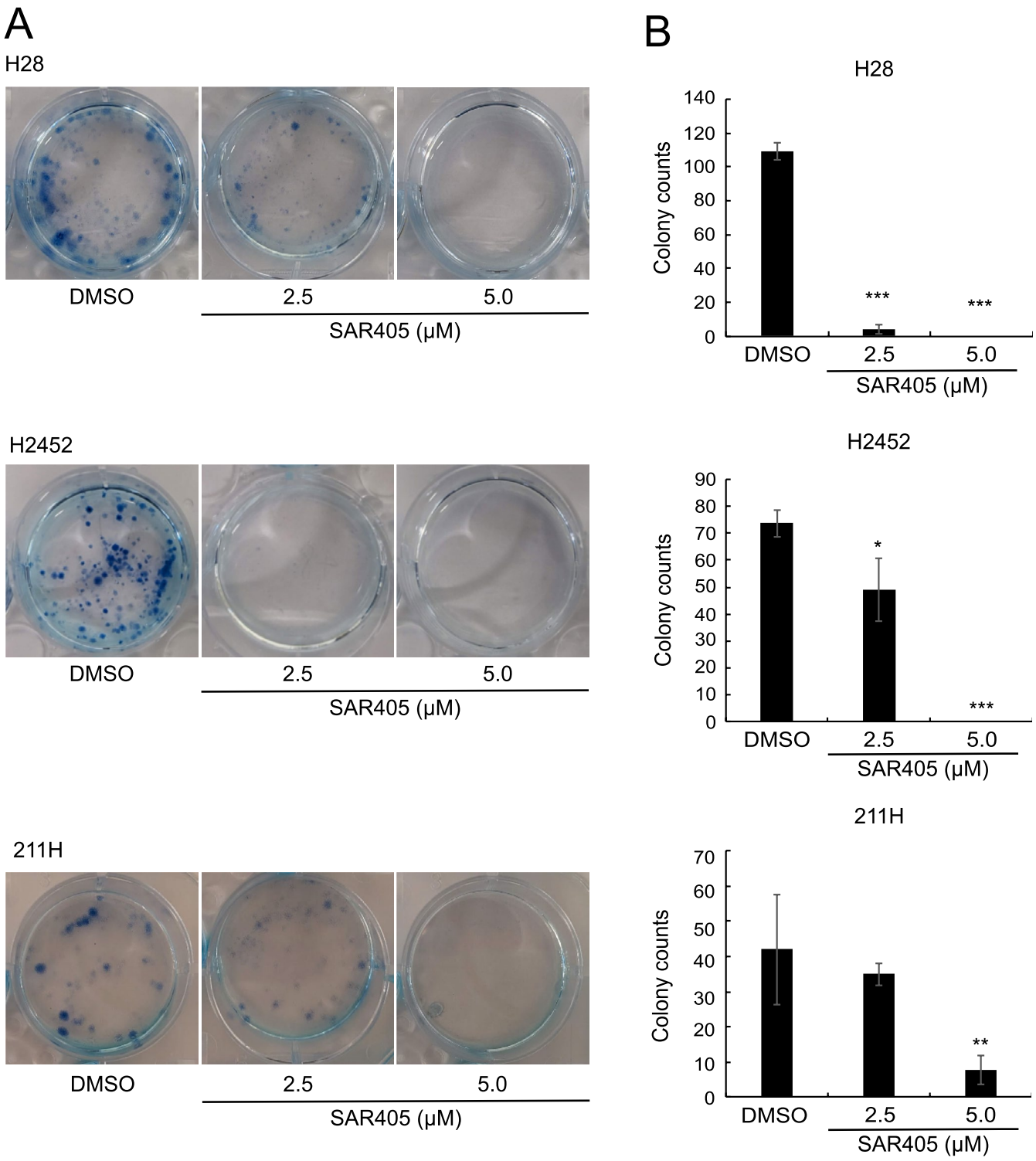


FIGURE 3 | Effects of SAR405 on colony formation by mesothelioma cells. (A) Cells were spread on dishes and cultured for 10 days in 211H and for 14 days in H28 and H2452 with 2.5–5.0 μM SAR405 or dimethyl sulfoxide (DMSO). (B) Mean (±SD) number of colonies formed by each mesothelioma cell line. *$p < 0.05$, **$p < 0.01$, ***$p < 0.001$ compared with DMSO.

pleural mesothelioma, fluorescence microscopy (Figure 7A) and flow cytometry (Figure 7B) were used to investigate the effects of cisplatin alone on autophagy in pleural mesothelioma cells transfected with the pMRX-IP-GFP-LC3-RFP-LC3ΔG plasmid. GFP-LC3 fluorescence was decreased in cisplatin compared with control (normal saline); specifically, the GFP/RFP ratio decreased following the addition of 5.0 μM cisplatin to H28 and 211H cells and 0.5 μM cisplatin to H2452 cells. Although cisplatin decreased p62 expression in a concentration-dependent manner in H2452 cells, it had no effect on p62 expression in H28 and 211H cells (Figure S1). The LC3B band was difficult to detect in all mesothelioma cell lines, suggesting that autophagy was scarcely induced in these cells under steady state conditions. Thus, even using

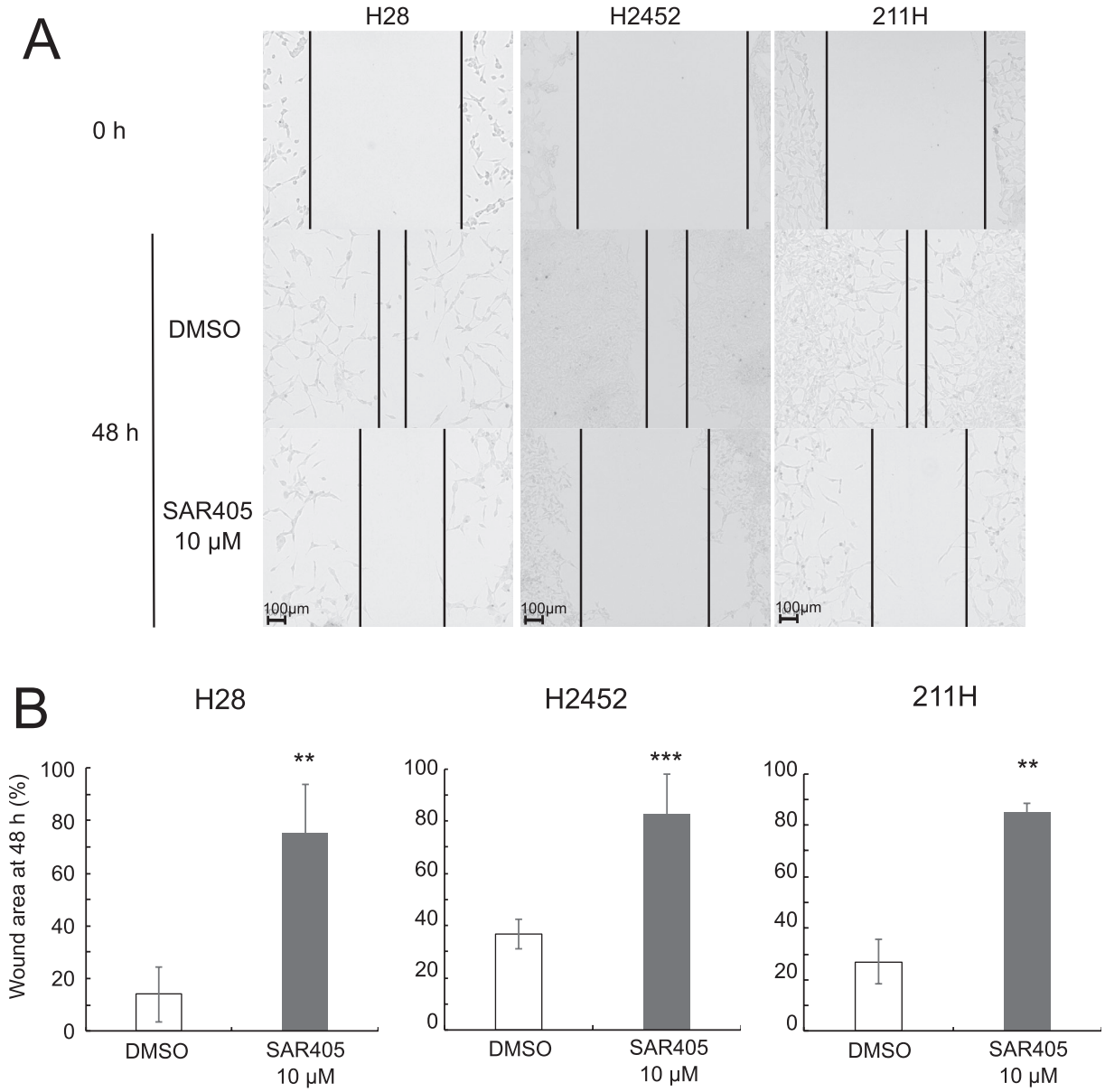


FIGURE 4 | Effects of SAR405 on cell migration/invasion. (A) Cell invasion of H28, H2452, and 211H mesothelioma cells was measured using a scratch wound healing assay. A single scratch was made in the center of the confluent cell monolayer, and cells were then treated with 10.0 μM SAR405 or dimethyl sulfoxide (DMSO) as a control. Cell invasion was monitored for 48 h and visualized by light microscopy. (B) Wound area remaining at 48 h in cells treated with DMSO or 10.0 μM SAR405. Data are the mean ± SD of three independent experiments. $^{**}p < 0.01$, $^{***}p < 0.001$ compared with DMSO.

chloroquine to evaluate changes in autophagy after cisplatin administration was difficult (data not shown).

3.6 | Effects of the Combination of SAR405 and Cisplatin

The cell viability of H28 and 211H cells, but not H2452 cells, appeared to be suppressed by the combination of cisplatin and SAR405 (Figure 8A). However, analysis using SynergyFinder (version 3.0) showed that the ZIP synergy score was less than −10 in all mesothelioma cell lines, indicating an antagonistic effect for the combination of cisplatin and SAR405. ZIP synergy scores for the other VPS34 inhibitors, namely PIK-III and Vps34-IN-1, were less than −10 for both in H28 cells, between −10 and 10 for both in H2452 cells, and between −10 and 10 for PIK-III and less than −10 for Vps34-IN-1 in 211H cells (Figure 8B). These results indicate that the combination of cisplatin and VPS34 inhibitors exhibits weak additive or antagonistic effects.

3.7 | Effects of SAR405 in a 3D Spheroid Model

Based on our in vitro findings, we further evaluated the antitumor effects of SAR405 using a three-dimensional (3D) spheroid model to better recapitulate in vivo tumor architecture. Quantitative analysis of the projected spheroid area revealed

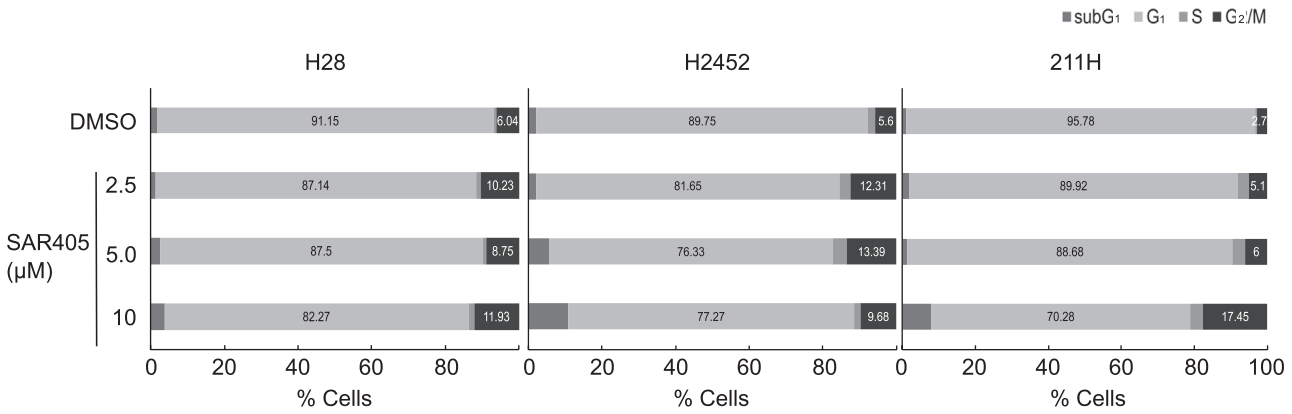


FIGURE 5 | Effects of SAR405 on the cell cycle in H28, H2452, and 211H mesothelioma cells. SAR405 induced G_2/M cycle arrest in pleural mesothelioma cells: The proportion of cells in the G_2/M phase was higher after culture with 2.5–10.0 μM SAR405 for 48 h than after culture with dimethyl sulfoxide (DMSO) as the control.

that treatment with SAR405 at 10 μM significantly reduced spheroid size in the H28 cell line compared with the DMSO control. In contrast, although a decreasing trend in spheroid area was observed in the H2452 and 211H cell lines, these changes did not reach statistical significance (Figure 9).

4 | Discussion

This study demonstrated that inhibition of VPS34 by SAR405 significantly suppressed cell viability in pleural mesothelioma cell lines. Autophagy, a crucial cellular process, is regulated by autophagy-related genes and proteins, including Beclin1 (BECN1), VPS34, UV radiation resistance-associated gene protein (UVRAG), vacuole membrane protein 1 (VMP1), and tumor protein p53 inducible nuclear protein 2 (TP53INP2). Of these autophagy-related genes, VPS34 is the sole class III lipid kinase responsible for generating phosphatidylinositol 3-phosphate, a lipid essential for the initiation of autophagosomal biogenesis [22]. The therapeutic potential of VPS34 inhibitors such as SAR405 lies in their ability to control autophagy, which has been implicated in cancer progression. Indeed, SAR405 has been reported to suppress tumor growth as a single agent in various cancers, including colorectal cancer [23], melanoma [23], head and neck squamous cancer [24], and breast cancer [25].

Autophagy is also known to play a significant role in cell cycle regulation. During cell cycle progression, autophagy occurs predominantly in the G_1 and S phases [26]. In pleural mesothelioma cells, administration of the anti-CD26 monoclonal antibody YS110 has been shown to induce G_2/M phase arrest [27]. Similarly, the combination of infigratinib (a fibroblast growth factor receptor inhibitor) and PKI-402 (a phosphatidylinositol 3-kinase [PI3K]/mammalian target of rapamycin inhibitor) inhibited autophagy and caused G_2/M phase arrest in cholangiocarcinoma cells [28]. In the present study, SAR405-induced inhibition of autophagy in pleural mesothelioma cells led to cell cycle arrest in the G_2/M phase. A previous study showed that phosphorylation of VPS34 at Thr^{159} by CDK1, a kinase controlling the G_2/M phase via cyclin A/B, disrupts its interaction with BECN1, thereby inhibiting autophagy [29]. These findings, together with those of the present study, suggest that VPS34 plays a pivotal role in coordinating autophagy and cell cycle regulation. Further research is required to elucidate the precise mechanisms involved.

Cancer cell migration, a key step in metastasis, allows cancer cells to invade surrounding tissues and establish contact with other tumor cells. This process is associated with a high risk of tumor recurrence if not adequately controlled [30]. In the present study, SAR405 significantly inhibited scratch wound closure by pleural mesothelioma cells, demonstrating its potential to suppress tumor cell migration and prevent metastasis. Colony formation is another critical step in tumor metastasis. This process is challenging for metastatic cells because the microenvironment of target organs differs significantly from that of the primary tumor [31]. Previous studies have reported that pharmacological inhibition of autophagy suppresses colony formation. For example, resveratrol, a stilbenoid, was shown to induce autophagy-dependent cell death and inhibit colony formation by A549 lung cancer cells [32]. Similarly, the lysosomal autophagy inhibitor Lys05 inhibited colony formation by clear cell ovarian carcinoma cells [33], and quinacrine inhibited colony formation by pleural mesothelioma cells [34]. Consistent with these findings, we showed that SAR405 significantly inhibited colony formation by pleural mesothelioma cells, further underscoring the therapeutic potential of autophagy inhibition in reducing metastatic capability.

In addition to the effects on viability and metastasis, SAR405 was found to induce apoptosis in H2452 pleural mesothelioma cells. The relationship between autophagy and apoptosis is complex and context dependent (i.e., autophagy can either promote or inhibit apoptosis depending on cell type and stress conditions) [35]. In pleural mesothelioma cells, quinacrine has been reported to inhibit autophagy and induce apoptosis [34]. Other studies have shown that combinations of cisplatin with the selective Janus tyrosine kinases 2/signal transducer and activator of transcription 3 inhibitor JSI-124 [36], sulforaphane [37], or the selective CDK4/6 inhibitor abemaciclib [38] can induce both autophagy and apoptosis. Conversely, the combination of simvastatin (a 3-hydroxy-3-methylglutaryl coenzyme A reductase inhibitor) with pemetrexed was found to induce autophagy and inhibit apoptosis [39]. Regarding SAR405, it has been reported that its combination

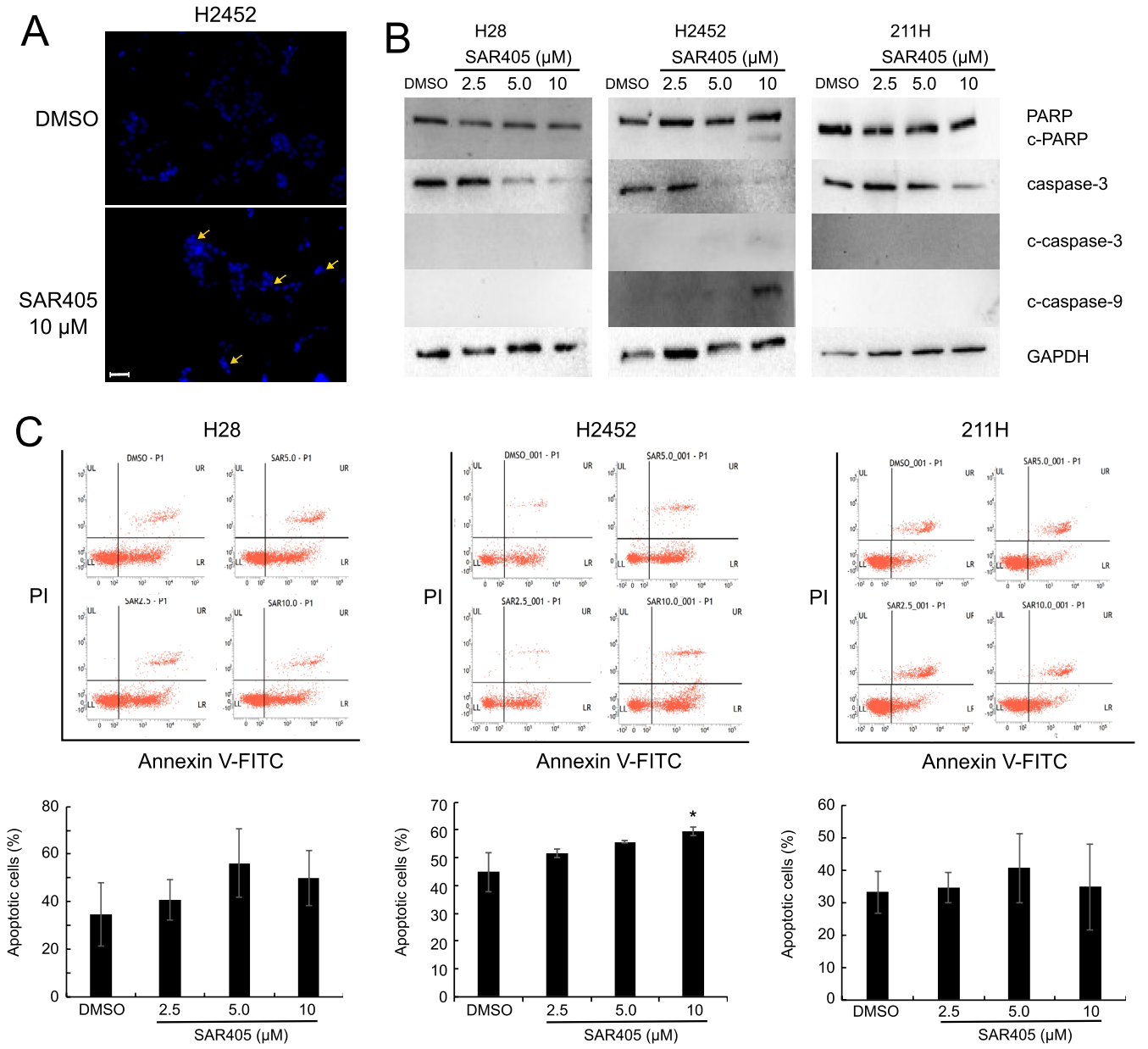


FIGURE 6 | Effects of SAR405 on apoptosis of H2452 pleural mesothelioma cells. (A) Mesothelioma H2452 cells were treated with 10.0 μM SAR405 for 48 h, stained with Hoechst 33342 to assess nuclear morphology, and visualized under a fluorescence microscope. Arrows indicate apoptotic cells. Scale bars = 200 μm. (B) Mesothelioma cells were treated with 2.5–10.0 μM SAR405 or dimethyl sulfoxide (DMSO) for 24 h and subjected to western blotting analysis to determine the expression of poly ADP-ribose polymerase (PARP), cleaved (c-) PARP, caspase-3, c-caspase-3, and c-caspase-9. GAPDH, glyceraldehyde-3-phosphate dehydrogenase. (C) The induction of apoptosis by SAR405 was evaluated using flow cytometry. Apoptotic cells were stained with annexin-V/fluorescein isothiocyanate (FITC) and propidium iodide (PI). Data are presented as the mean ± SD of three independent experiments. *$p < 0.05$ compared with DMSO.

with the selective cyclo-oxygenase 2 inhibitor celecoxib [40], or the type I PI3K knockdown agent EZN4150 [25], inhibits autophagy and induces apoptosis. Consistent with these findings, we observed induction of apoptosis by SAR405 in H2452 cells. However, apoptosis was not induced in H28 or 211H cells. Evaluation of differences in genetic backgrounds and anti-apoptotic pathways may partially explain the cell-line specific apoptotic responses to autophagy inhibition. Although *TP53* mutations are generally rare in pleural mesothelioma, homozygous deletion of the *CDKN2A* locus which encodes $p16^{INK4a}$ and $p14^{ARF}$, occurs in more than 70% of cases. $p14^{ARF}$ stabilizes p53 by promoting the degradation of MDM2; therefore, deletion of this site results in attenuation of p53 function [41]. Although, H28 and 211H cells harbor wild-type p53, H2452 cells contain a truncated form of p53, which may lead to a greater loss of function compared with the other two cell lines [42]. These genetic differences may underlie the observed variation in apoptotic response to SAR405. Moreover, previous studies have reported that H2452 cells treated with RITA, a small-molecule reactivator of p53, exhibit stronger apoptosis induction than pleural mesothelioma cell lines expressing wild-type p53 [43]. Given that autophagy is known, in certain context, to promote tumorigenesis in part through suppression of p53 activity [44], the interaction between autophagy inhibition and p53 status in pleural mesothelioma warrants further investigation. Gene expression

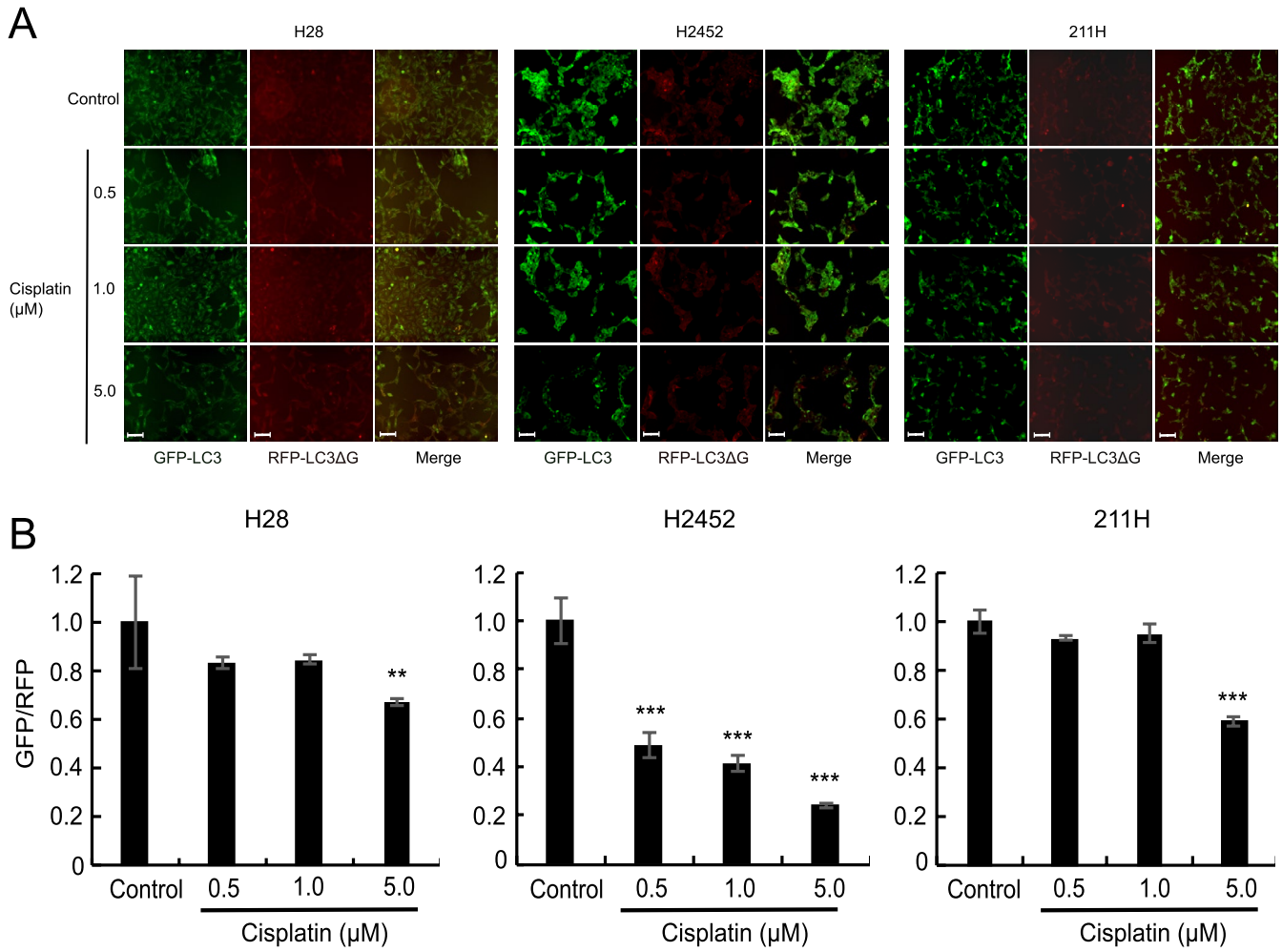


FIGURE 7 | Effects of cisplatin on autophagy in pleural mesothelioma cells. (A) Fluorescence microscopy findings for transfected mesothelioma cells cultured for 24 h with 0.5–5.0 μM cisplatin or control (normal saline). Scale bars = 200 μm. (B) Signal intensities of green fluorescent protein (GFP) and red fluorescent protein (RFP) were measured by flow cytometry after 24 h culture of H28, H2452, and 211H cells with 0.5–5.0 μM cisplatin or control (normal saline), and the GFP/RFP ratio was determined. Data are the mean ± SD of three independent experiments. $^{**}p < 0.01$, $^{***}p < 0.001$ compared with control.

data for BECN1 and apoptosis related protein (Bcl-2, Bcl-xL, Mcl-1, Bak, and Bax) data in mesothelioma cell lines were obtained from the DepMap portal (https://depmap.org/portal/) using RNA-seq datasets. Corresponding gene expression levels (BECN1, BCL2, BCL2L1, MCL1, BAK1, and BAX) were compared among H2452, H28, and 211H cells. Notably, the expression level of BCL2, which encodes an anti-apoptotic protein, was relatively lower in H2452 cells than in H28 and 211H cells ($\log_2$-transformed transcripts per million [TPM + 1]: 1.21, 2.16, and 2.37 in H2452, H28, and 211H, respectively). BECN11, an essential autophagy-related protein, is negatively regulated through its interaction with Bcl-2 or Bcl-xL [45]. Therefore, H2452 may be more sensitive to disruptions in autophagic regulation, while their anti-apoptotic capacity may be relatively limited. BRCA1-associated protein 1 (BAP-1) is mutated in more than 60% of malignant pleural mesotheliomas. H2452 and H28 cells harbor BAP1 loss, whereas 211H retain BAP1 expression [46]. Recently, in BAP1-mutant cancer cells, BAP1 loss has been shown to transcriptionally upregulate the proto-oncogene SRC, leading to SRC-mediated phosphorylation and inactivation of BECN1 [47]. In that study, treatment with SRC inhibitors and autophagy-induced agents suppressed tumor growth in uveal melanoma and clear-cell renal cell carcinoma models. The authors also noted that autophagy inhibitors have been tested in combination with other therapies in multiple clinical trials; however, these resulted in significant adverse events and toxicities. Based on these findings, they proposed therapeutic strategies combining SRC inhibition with autophagy induction, including compounds that disrupt the binding of Bcl-2 to BECN1, for patients with BAP-1-mutant cancers. Our previous report demonstrated that VER-155008, an HSP70 inhibitor, suppressed cell growth in pleural mesothelioma cell lines, including H2452, H28, and 211H, as examined in the present study, accompanied by reduced phosphorylated AKT expression and enhanced macroautophagy [16]. In that study, it was not possible to determine whether autophagy functioned in cytotoxic or cytoprotective manner. Together with the present findings using the VPS34 inhibitor SAR405, these results suggest that mesothelioma cells may be vulnerable to both excessive induction and excessive suppression of autophagy, likely due to limited autophagic adaptability. Importantly, although both H2452 and H28 cells lack BAP1 expression, only H2452 cells underwent apoptosis upon VPS34 inhibition. Our data suggest that additional factors, such as differences in autophagic adaptability,

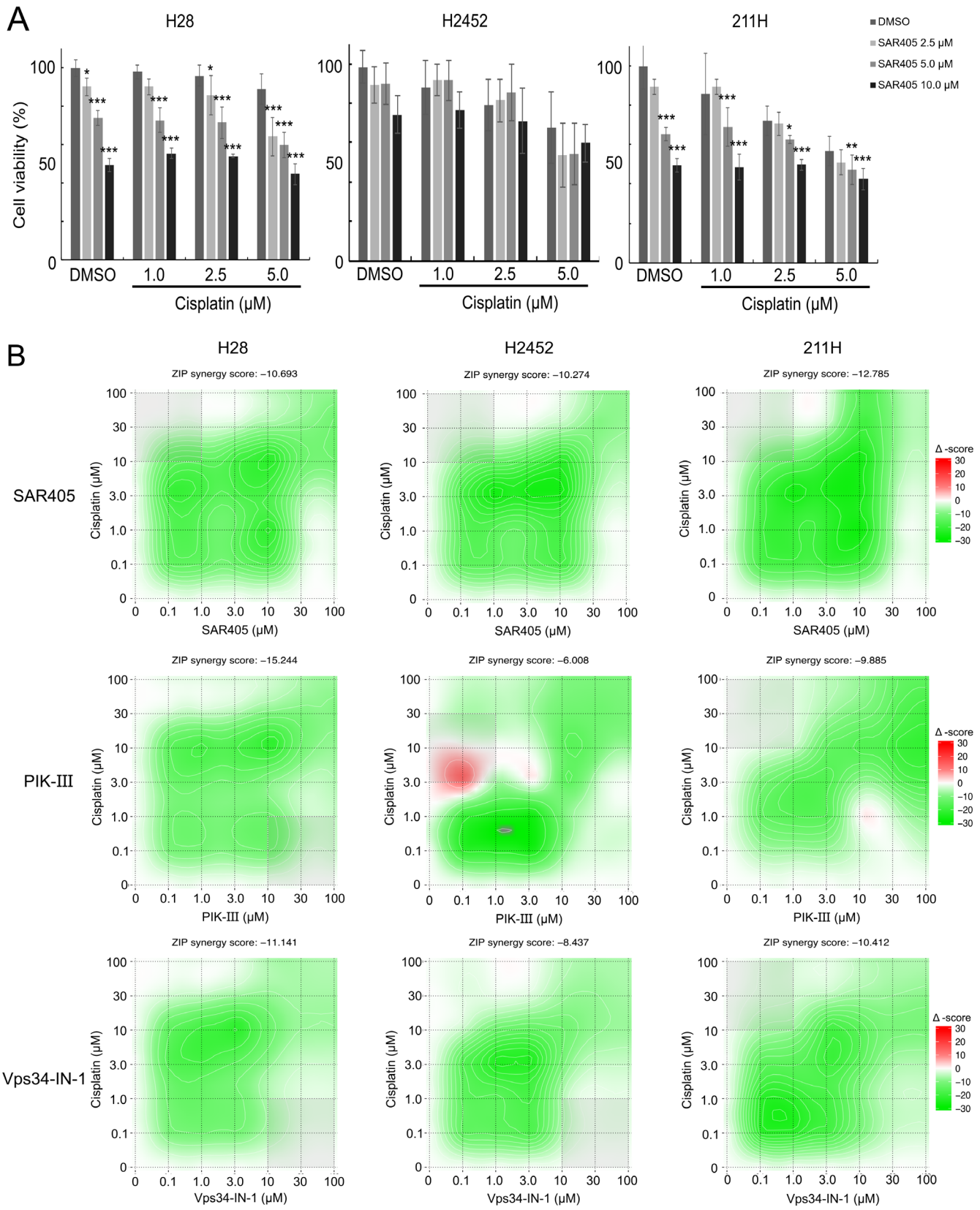


FIGURE 8 | Legend on next page.

or Bcl-2 family-mediated apoptotic regulation, may influence cell fate following disruption of autophagy in BAP1-deficint cancer cells. Collectively, the selective induction of apoptosis observed in H2452, but not in H28 or 211H cells, may be partially attributed to genetic differences in p53 status and lower expression of BCL2, an anti-apoptotic protein that also regulates the essential autophagy protein BECN1. Despite sharing BAP1 loss, H28 cells did not undergo apoptosis, suggesting that dependency on autophagic

FIGURE 8 | No synergistic effect was seen for the combination of SAR405 and cisplatin. (A) Mesothelioma cells were cultured for 72 h with 1.0–5.0 μM cisplatin, 2.5–10.0 μM SAR405, or dimethyl sulfoxide (DMSO) as a control. Cell viability was assessed by the reduction of water-soluble tetrazolium 8 (WST-8). The results show the proportion of viable cells after 72 h treatment with either cisplatin combined with SAR405 or DMSO. The proportion of viable cells was lower after combined treatment with cisplatin and SAR405 than after treatment with DMSO. Data are the mean ± SD of three independent experiments. *$p < 0.05$, **$p < 0.01$, ***$p < 0.001$ compared with control. (B) Drug interactions of cisplatin with either SAR405, PIK-III, or Vps34-IN-1 in mesothelioma cell lines. H28, H2452, and 211H cells were cultured for 72 h with 0.1–100 μM cisplatin and 0.1–100 μM SAR405, PIK-III, or Vps34-IN-1. Drug interactions were evaluated using SynergyFinder (version 3.0) using the zero interaction potency (ZIP) model. A ZIP synergy score > 10 is considered synergistic; a score between −10 and 10 is considered additive; and a score less than −10 is considered antagonistic.

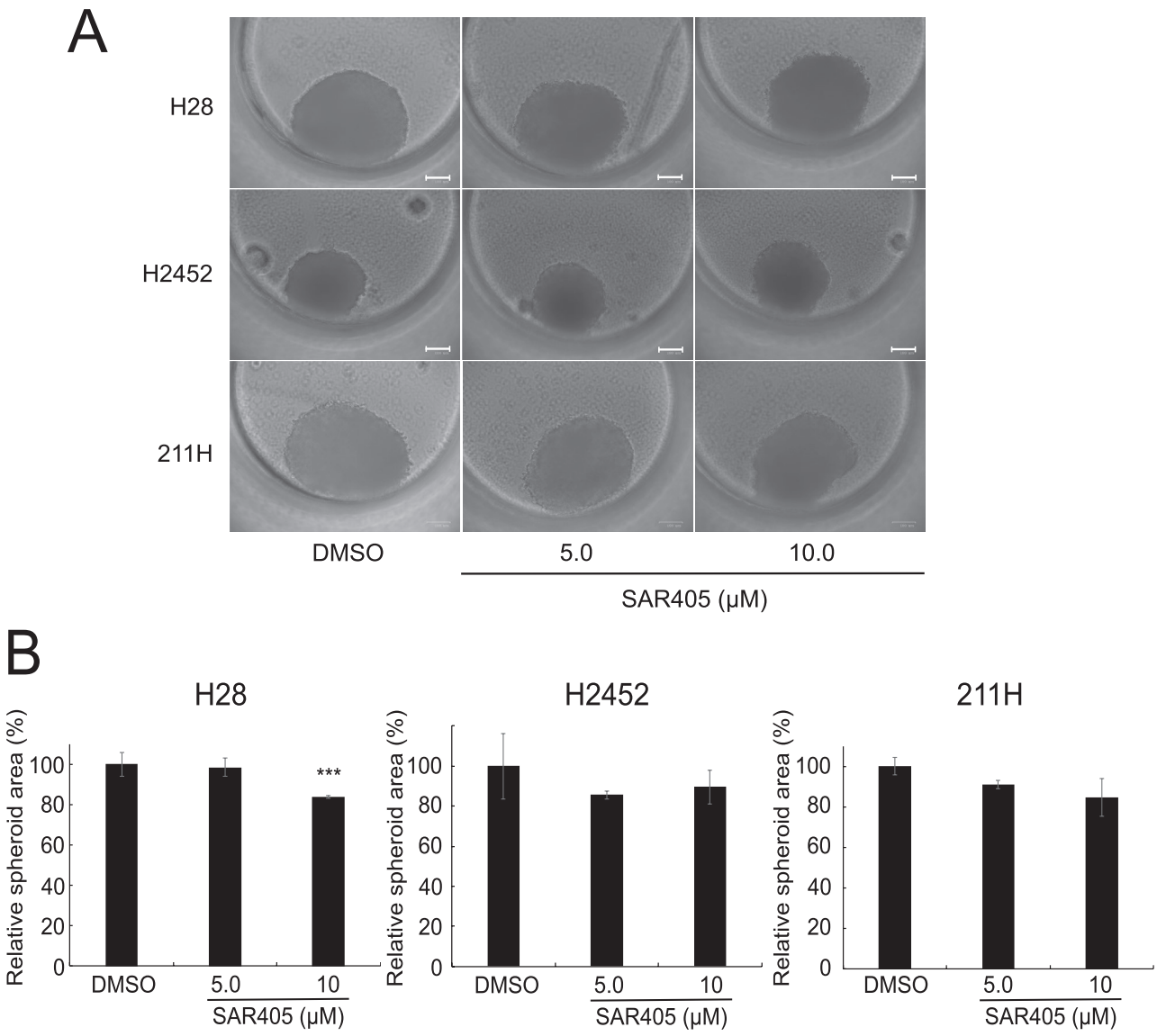


FIGURE 9 | Effects of SAR405 in a 3D spheroid model. (A) Spheroid cells were cultured for 72 h with 5.0–10.0 μM SAR405, or dimethyl sulfoxide (DMSO) as a control. Spheroids were imaged using a ZOE Fluorescent Cell Imager. Scale bars = 100 μm. (B) Spheroid size was quantified as projected area using ImageJ software version 1.54 g. Data are the mean ± SD of three independent experiments. ***$p < 0.001$ compared with control.

imbalance among BAP-1 mutant cancers varies according to cancer type and specific genetic background. These mechanisms are intriguing and intricate, and warrant further investigation.

Cisplatin remains a cornerstone therapy for pleural mesothelioma, even with the advent of immune checkpoint inhibitors. Previous studies have reported that cisplatin induces autophagy in pleural mesothelioma cell lines, but only in combination with other agents [37, 38]. In the present study, cisplatin alone weakly induced autophagy, as detected using a novel plasmid-based autophagy flux assay (pMRX-IP-GFP-LC3-RFP-LC3ΔG), which is more sensitive than the conventional assay with western blotting analysis [17]. Given that autophagy is known to be induced by serum starvation or amino acid starvation, it is difficult to measure autophagy in a steady state [48]. To evaluate autophagy status, the dynamic

range of autophagic flux is measured using chloroquine or bafilomycin A1. However, the present study revealed that it is difficult to detect cisplatin-induced autophagy in pleural mesothelioma cell lines based on p62 expression determined by western blot analysis, even with measurement of autophagic flux using chloroquine. The plasmid-transfected pleural mesothelioma cell lines for autophagy induction enabled us to detect subtle cisplatin-induced autophagy, which was not seen with western blotting.

The combination of SAR405 and cisplatin did not exhibit additive or synergistic effects in our experiments. These findings may suggest two contradictory conclusions: one is that cisplatin-induced autophagy may exert a weak cytotoxic effect and the other is that the extent of autophagy induced by cisplatin is so limited that its inhibition, even in combination with an autophagy inhibitor, fails to produce a synergistic antitumor effect in pleural mesothelioma cells. Cisplatin induces cytotoxicity primarily through the formation of several types of DNA adducts (including monoadducts, intrastrand crosslinks, and DNA-protein crosslinks), which activates the DNA damage response and apoptosis [49]. Given that autophagy, the DNA damage response, and apoptosis are interconnected through numerous protein interactions and are mutually regulated at multiple levels, the stage of autophagy inhibition and the specific molecular targets involved may produce divergent effects on cell viability. In general, cisplatin-induced autophagy has been reported to play a cytoprotective role; however, accumulating evidence indicates that cisplatin can also induce cytotoxic or non-protective autophagy in certain contexts. For example, in the non-small cell lung cancer cell line H460 (p53 wild-type), cisplatin-induced autophagy has been reported to be non-protective [50]. Furthermore, DNA damage response–related pathways, including p53, ATM/ATR, and MAPK signaling, have been implicated in modulating both the induction of autophagy and cellular sensitivity to cisplatin [51]. Similarly, the effects of combining SAR405 with cisplatin appear to be context-dependent: while enhanced cytotoxicity has been observed in both cisplatin-sensitive and cisplatin-resistant urothelial carcinoma cell lines [52], no such enhancement was reported in malignant rhabdoid tumor cells [53]. These observations suggest that autophagy under cisplatin treatment may function not as a survival pathway but rather as a cell death–promoting mechanism under specific cellular conditions. Considering these findings, it is possible that cisplatin-induced autophagy acts in a cytotoxic, rather than cytoprotective, manner in mesothelioma cell lines. In any case, these findings highlight the need for further research to determine how autophagy regulation varies according to cancer type and therapeutic context.

In the 3D spheroid model, treatment with SAR405 significantly inhibited spheroid expansion in H28 cell line, whereas only a non-significant decreasing trend was observed in H2452 and 211H cell lines. Although the mechanisms underlying these cell line–specific differences remain unclear, previous studies have reported that inhibition of early-stage autophagy using a single agent does not consistently exert antitumor effects in pleural mesothelioma cell lines [54]. Given the relatively high IC_{50} of SAR405, identifying combination strategies that enhance its antitumor efficacy represents an important direction for future research.

SAR405 faces challenges such as its poor hydrophilicity, limited stability, and low bioavailability, which are commonly encountered challenges with small-molecule kinase inhibitors. These properties necessitate frequent or high-dose administration for sustained therapeutic exposure. To address these concerns, some studies have shown that SAR405-loaded chitosan nanoparticles enhance cellular uptake and increase cytotoxicity in A549 lung cancer cells [55]. In addition, a low-intensity focused ultrasound (LIFU)–responsive phase-change nanodroplet platform (SP@Lip-PEG) has been developed to improve intratumoral accumulation and triggered release of SAR405 [56]. Applying these delivery strategies to pleural mesothelioma could improve its clinical applicability. Moreover, immune checkpoint inhibitors have recently become an integral component of pleural mesothelioma treatment. One of the major limitations of anti–PD-1/PD-L1 therapy is insufficient infiltration of effector T cells into the tumor microenvironment. Notably, pharmacological inhibition of VPS34 using SAR405 in melanoma and colon cancer has been shown to enhance infiltration of NK cells, $CD8^+$ T cells, and $CD4^+$ effector T cells, reduce tumor growth, and prolong survival in mouse models [23]. Considering these findings, combining VPS34 inhibition with immune checkpoint inhibitors therapy may represent a promising multimodal approach for pleural mesothelioma.

In conclusion, this study provides evidence that SAR405 has the potential to inhibit autophagy, to suppress cell viability and metastasis, and to induce apoptosis in pleural mesothelioma cells. Future investigations should focus on combining cisplatin with therapeutic agents that target distinct stages of autophagy or using genetic approaches to suppress autophagy-related genes, and on identifying the combination partners, including immunotherapeutic agents, that enhance the antitumor efficacy of SAR405. Such studies will deepen our understanding of the role of autophagy in pleural mesothelioma and contribute to the development of more effective therapeutic strategies.

Author Contributions

All authors had full access to the data in the study and take responsibility for the integrity of the data and the accuracy of the data analysis. Conceptualization: Y. Kuwabara, K. Sakai, and K.U.; Methodology: Y. Kuwabara, K. Sakai, and K.U.; Investigation: Y. Kuwabara, K. Sakai, K. Shiraishi, I.M., S.I., S.Y., M.A., T.T., Y. Kawano, H.N., M.T-.S., Y. Kobayashi, S. Kikuchi, Y.H., H.K., and G.M.; Formal analysis: Y. Kuwabara, and K. Sakai; Resources: Y. Kuwabara, K. Sakai, H.N., and H.K.; Writing – original draft: Y. Kuwabara, K. Sakai, and K.U.; Writing – review and editing, Y. Kuwabara, N.K., and K.U.; Visualization: Y. Kuwabara, and K. Sakai; Supervision: K.U.; Funding acquisition: N.K., and K.U.

Acknowledgments

The authors thank Dr. Tai Hato and Professor Mitsuo Nakayama (Department of General Thoracic Surgery, Saitama Medical Center, Saitama Medical University) for their guidance of the use of the BZ-X810 fluorescence microscope. This research was supported by Ochiai Memorial Award Research 2024 from the Saitama Medical University Alumni Association and an internal (05-F-1-12) from Saitama Medical University, Eli Lilly Japan KK Innovation Research 2025, and JSPS KAKENHI JP 24K11375.

Funding

This work was supported by Saitama Medical University, 05-F-1-12. JSPS KAKENHI, JP 24K11375. Eli Lilly Japan KK Innovation Research 2025.

Conflicts of Interest

The authors declare no conflicts of interest.

Data Availability Statement

The data that support the findings of this study are available from the corresponding author upon reasonable request.

References

1. T. Murayama, K. Takahashi, Y. Natori, and N. Kurumatani, "Estimation of Future Mortality From Pleural Malignant Mesothelioma in Japan Based on an Age-Cohort Model," *American Journal of Industrial Medicine* 49, no. 1 (2006): 1–7.

2. B. Levine and G. Kroemer, "Autophagy in the Pathogenesis of Disease," *Cell* 132, no. 1 (2008): 27–42.

3. N. Mizushima, "The Role of the Atg1/ULK1 Complex in Autophagy Regulation," *Current Opinion in Cell Biology* 22, no. 2 (2010): 132–139.

4. J. D. Rabinowitz and E. White, "Autophagy and Metabolism," *Science* 330, no. 6009 (2010): 1344–1348.

5. E. White, "Deconvoluting the Context-Dependent Role for Autophagy in Cancer," *Nature Reviews. Cancer* 12, no. 6 (2012): 401–410.

6. S. Wilkinson and K. M. Ryan, "Autophagy: An Adaptable Modifier of Tumourigenesis," *Current Opinion in Genetics & Development* 20, no. 1 (2010): 57–64.

7. O. Nagano, S. Okazaki, and H. Saya, "Redox Regulation in Stem-Like Cancer Cells by CD44 Variant Isoforms," *Oncogene* 32, no. 44 (2013): 5191–5198.

8. R. Chavez-Dominguez, M. Perez-Medina, J. S. Lopez-Gonzalez, M. Galicia-Velasco, and D. Aguilar-Cazares, "The Double-Edge Sword of Autophagy in Cancer: From Tumor Suppression to Pro-Tumor Activity," *Frontiers in Oncology* 10 (2020): 578418.

9. Y. S. Abd El-Aziz, M. J. McKay, M. P. Molloy, et al., "Inhibition of Autophagy Initiation: A Novel Strategy for Oral Squamous Cell Carcinomas," *Biochimica et Biophysica Acta, Molecular Cell Research* 1871, no. 2 (2024): 119627.

10. Y. S. Abd El-Aziz, J. Gillson, P. J. Jansson, and S. Sahni, "Autophagy: A Promising Target for Triple Negative Breast Cancers," *Pharmacological Research* 175 (2022): 106006.

11. X. Song, D. H. Lee, A. K. Dilly, et al., "Crosstalk Between Apoptosis and Autophagy Is Regulated by the Arginylated BiP/Beclin-1/p62 Complex," *Molecular Cancer Research* 16, no. 7 (2018): 1077–1091.

12. S. Magnano, P. Hannon Barroeta, R. Duffy, J. O'Sullivan, and D. M. Zisterer, "Cisplatin Induces Autophagy-Associated Apoptosis in Human Oral Squamous Cell Carcinoma (OSCC) Mediated in Part Through Reactive Oxygen Species," *Toxicology and Applied Pharmacology* 427 (2021): 115646.

13. R. B. Melles and M. F. Marmor, "The Risk of Toxic Retinopathy in Patients on Long-Term Hydroxychloroquine Therapy," *JAMA Ophthalmol* 132, no. 12 (2014): 1453–1460.

14. F. Wolfe and M. F. Marmor, "Rates and Predictors of Hydroxychloroquine Retinal Toxicity in Patients With Rheumatoid Arthritis and Systemic Lupus Erythematosus," *Arthritis Care & Research (Hoboken)* 62, no. 6 (2010): 775–784.

15. T. T. Shi, X. X. Yu, L. J. Yan, and H. T. Xiao, "Research Progress of Hydroxychloroquine and Autophagy Inhibitors on Cancer," *Cancer Chemotherapy and Pharmacology* 79, no. 2 (2017): 287–294.

16. K. Sakai, M. Inoue, S. Mikami, et al., "Functional Inhibition of Heat Shock Protein 70 by VER-155008 Suppresses Pleural Mesothelioma Cell Proliferation via an Autophagy Mechanism," *Thorac Cancer* 12, no. 4 (2021): 491–503.

17. T. Kaizuka, H. Morishita, Y. Hama, et al., "An Autophagic Flux Probe That Releases an Internal Control," *Molecular Cell* 64, no. 4 (2016): 835–849.

18. C. A. Schneider, W. S. Rasband, and K. W. Eliceiri, "NIH Image to ImageJ: 25 Years of Image Analysis," *Nature Methods* 9, no. 7 (2012): 671–675.

19. Y. Kanda, "Investigation of the Freely Available Easy-To-Use Software 'EZR' for Medical Statistics," *Bone Marrow Transplantation* 48, no. 3 (2013): 452–458.

20. B. Yadav, K. Wennerberg, T. Aittokallio, and J. Tang, "Searching for Drug Synergy in Complex Dose-Response Landscapes Using an Interaction Potency Model," *Computational and Structural Biotechnology Journal* 13 (2015): 504–513.

21. P. Indovina, E. Marcelli, D. Di Marzo, et al., "Abrogating G2/M Checkpoint Through WEE1 Inhibition in Combination With Chemotherapy as a Promising Therapeutic Approach for Mesothelioma," *Cancer Biology & Therapy* 15, no. 4 (2014): 380–388.

22. L. Chen, T. Gao, P. Zhou, et al., "Recent Advances of Vacuolar Protein-Sorting 34 Inhibitors Targeting Autophagy," *Bioorganic Chemistry* 143 (2024): 107039.

23. M. Z. Noman, S. Parpal, K. van Moer, M. Xiao, Y. Yu, and J. Viklund, "Inhibition of Vps34 Reprograms Cold Into Hot Inflamed Tumors and Improves Anti-PD-1/PD-L1 Immunotherapy," *Science Advances* 6, no. 18 (2020): eaax7881.

24. J. New, L. Arnold, M. Ananth, et al., "Secretory Autophagy in Cancer-Associated Fibroblasts Promotes Head and Neck Cancer Progression and Offers a Novel Therapeutic Target," *Cancer Research* 77, no. 23 (2017): 6679–6691.

25. C. D. Young, C. L. Arteaga, and R. S. Cook, "Dual Inhibition of Type I and Type III PI3 Kinases Increases Tumor Cell Apoptosis in HER2+ Breast Cancers," *Breast Cancer Research* 17 (2015): 148.

26. D. V. Ziegler, K. Huber, and L. Fajas, "The Intricate Interplay Between Cell Cycle Regulators and Autophagy in Cancer," *Cancers (Basel)* 14, no. 1 (2021): 153.

27. M. Hayashi, H. Madokoro, K. Yamada, et al., "A Humanized Anti-CD26 Monoclonal Antibody Inhibits Cell Growth of Malignant Mesothelioma via Retarded G2/M Cell Cycle Transition," *Cancer Cell International* 16 (2016): 35.

28. C. H. Chen, C. A. Changou, T. H. Hsieh, et al., "Dual Inhibition of PIK3C3 and FGFR as a New Therapeutic Approach to Treat Bladder Cancer," *Clinical Cancer Research* 24, no. 5 (2018): 1176–1189.

29. T. Furuya, M. Kim, M. Lipinski, J. Li, D. Kim, and T. Lu, "Negative Regulation of Vps34 by Cdk Mediated Phosphorylation," *Molecular Cell* 38, no. 4 (2010): 500–511.

30. Y. Nomura, H. Tashiro, and K. Hisamatsu, "In Vitro Clonogenic Growth and Metastatic Potential of Human Operable Breast Cancer," *Cancer Research* 49, no. 19 (1989): 5288–5293.

31. T. Schild, V. Low, J. Blenis, and A. P. Gomes, "Unique Metabolic Adaptations Dictate Distal Organ-Specific Metastatic Colonization," *Cancer Cell* 33, no. 3 (2018): 347–354.

32. S. K. Dasari, S. Bialik, S. Levin-Zaidman, et al., "Signalome-Wide RNAi Screen Identifies GBA1 as a Positive Mediator of Autophagic Cell Death," *Cell Death and Differentiation* 24, no. 7 (2017): 1288–1302.

33. L. DeVorkin, M. Hattersley, P. Kim, et al., "Autophagy Inhibition Enhances Sunitinib Efficacy in Clear Cell Ovarian Carcinoma," *Molecular Cancer Research* 15, no. 3 (2017): 250–258.

34. N. S. Kulkarni, B. Vaidya, V. Parvathaneni, D. Bhanja, and V. Gupta, "Repurposing Quinacrine for Treatment of Malignant Mesothelioma: In-Vitro Therapeutic and Mechanistic Evaluation," *International Journal of Molecular Sciences* 21, no. 17 (2020): 6306.

35. Q. Xie, Y. Liu, and X. Li, "The Interaction Mechanism Between Autophagy and Apoptosis in Colon Cancer," *Translational Oncology* 13, no. 12 (2020): 100871.

36. C. Zhang, Q. Sun, J. Zhao, et al., "JSI-124 Inhibits Cell Proliferation and Tumor Growth by Inducing Autophagy and Apoptosis in Murine Malignant Mesothelioma," *Molecular Carcinogenesis* 62, no. 12 (2023): 1888–1901.

37. Y. J. Lee and S. H. Lee, "Pro-Oxidant Activity of Sulforaphane and Cisplatin Potentiates Apoptosis and Simultaneously Promotes Autophagy in Malignant Mesothelioma Cells," *Molecular Medicine Reports* 16, no. 2 (2017): 2133–2141.

38. R. Terenziani, M. Galetti, S. la Monica, et al., "CDK4/6 Inhibition Enhances the Efficacy of Standard Chemotherapy Treatment in Malignant Pleural Mesothelioma Cells," *Cancers (Basel)* 14, no. 23 (2022): 5925.

39. K. E. Hwang, Y. S. Kim, J. W. Jung, et al., "Inhibition of Autophagy Potentiates Pemetrexed and Simvastatin-Induced Apoptotic Cell Death in Malignant Mesothelioma and Non-Small Cell Lung Cancer Cells," *Oncotarget* 6, no. 30 (2015): 29482–29496.

40. P. Zhou, Y. Li, B. Li, et al., "Autophagy Inhibition Enhances Celecoxib-Induced Apoptosis in Osteosarcoma," *Cell Cycle* 17, no. 8 (2018): 997–1006.

41. S. Romagnoli, E. Fasoli, V. Vaira, et al., "Identification of Potential Therapeutic Targets in Malignant Mesothelioma Using Cell-Cycle Gene Expression Analysis," *American Journal of Pathology* 174, no. 3 (2009): 762–770.

42. J. J. Manfredi, J. Dong, W. J. Liu, et al., "Evidence Against a Role for SV40 in Human Mesothelioma," *Cancer Research* 65, no. 7 (2005): 2602–2609.

43. D. Di Marzo, I. M. Forte, P. Indovina, et al., "Pharmacological Targeting of p53 Through RITA Is an Effective Antitumoral Strategy for Malignant Pleural Mesothelioma," *Cell Cycle* 13, no. 4 (2014): 652–665.

44. E. White, "The Role for Autophagy in Cancer," *Journal of Clinical Investigation* 125, no. 1 (2015): 42–46.

45. B. Levine, S. Sinha, and G. Kroemer, "Bcl-2 Family Members: Dual Regulators of Apoptosis and Autophagy," *Autophagy* 4, no. 5 (2008): 600–606.

46. S. Hakiri, H. Osada, F. Ishiguro, et al., "Functional Differences Between Wild-Type and Mutant-Type BRCA1-Associated Protein 1 Tumor Suppressor Against Malignant Mesothelioma Cells," *Cancer Science* 106, no. 8 (2015): 990–999.

47. S. Vega-Rubin-de-Celis, A. Kristani, M. Kudla, S. Mergener, A. Corrochano-Ruiz, and S. Larafa, "Autophagy Suppression via SRC Induction Represents a Therapeutic Vulnerability for," *Autophagy* 21, no. 12 (2025): 3324–3343.

48. N. Mizushima and L. O. Murphy, "Autophagy Assays for Biological Discovery and Therapeutic Development," *Trends in Biochemical Sciences* 45, no. 12 (2020): 1080–1093.

49. B. M. Gąsiorkiewicz, P. Koczurkiewicz-Adamczyk, K. Piska, and E. Pękala, "Autophagy Modulating Agents as Chemosensitizers for Cisplatin Therapy in Cancer," *Investigational New Drugs* 39, no. 2 (2021): 538–563.

50. N. H. Patel, J. Xu, T. Saleh, Y. Wu, S. Lima, and D. A. Gewirtz, "Influence of Nonprotective Autophagy and the Autophagic Switch on Sensitivity to Cisplatin in Non-Small Cell Lung Cancer Cells," *Biochemical Pharmacology* 175 (2020): 113896.

51. J. Xu and D. A. Gewirtz, "Is Autophagy Always a Barrier to Cisplatin Therapy?," *Biomolecules* 12, no. 3 (2022): 463.

52. D. Schlütermann, M. A. Skowron, N. Berleth, P. Böhler, J. Deitersen, and F. Stuhldreier, "Targeting Urothelial Carcinoma Cells by Combining Cisplatin With a Specific Inhibitor of the Autophagy-Inducing Class III PtdIns3K Complex," *Urologic Oncology* 36, no. 4 (2018): 160.e1–160.e13.

53. P. Hannon Barroeta, S. Magnano, M. J. O'Sullivan, and D. M. Zisterer, "Evaluation of Targeting Autophagy for the Treatment of Malignant Rhabdoid Tumours," *Cancer Treatment and Research Communications* 32 (2022): 100584.

54. C. Follo, Y. Cheng, W. G. Richards, R. Bueno, and V. C. Broaddus, "Inhibition of Autophagy Initiation Potentiates Chemosensitivity in Mesothelioma," *Molecular Carcinogenesis* 57, no. 3 (2018): 319–332.

55. M. N. Alamassi, S. L. Chia, C. A. C. Abdullah, and M. J. Masarudin, "Increased Efficacy of Biologics Following Inhibition of Autophagy in A549 Lung Cancer Cells in Bimodal Treatment of Doxorubicin and SAR405-Loaded Chitosan Nanoparticles," *OpenNano* 11 (2023): 100142.

56. N. Wu, Q. Zhang, R. Tang, et al., "Ultrasound Visualization of Spatiotemporal Autophagy-Regulated Nanodroplets for Amplifying ICB in Melanoma via Remodeling Tumor Inflammatory Microenvironment," *ACS Applied Materials & Interfaces* 17, no. 20 (2025): 29364–29378.

Supporting Information

Additional supporting information can be found online in the Supporting Information section. **Figure S1:** Cisplatin induced autophagy in pleural mesothelioma cells. H28, H2452, and 211H cells were treated with 1.0–5.0 μM cisplatin or control (normal saline) for 24 h and analyzed by western blotting analysis. Data are the mean ± SD of three independent experiments. $*p < 0.05$, $***p < 0.001$ compared with control.